2015-10

On learning time delays between the spikes from different input neurons in a biophysical model of a pyramidal neuron.

Koutsou, A

10.1016/j.biosystems.2015.08.005
Biosystems

To appear in BioSystems, doi:10.1016/j.biosystems.2015.08.005 (accepted in August 2015, in press)

On learning time delays between the spikes from different input neurons in a biophysical model of a pyramidal neuron

Achilleas Koutsou[a], Guido Bugmann[b], Chris Christodoulou[a,*]

[a] *Department of Computer Science, University of Cyprus*
P.O. Box 20537, 1678 Nicosia, Cyprus
[b] *School of Computing and Mathematics, Plymouth University*
Drake Circus, PL4 8AA Plymouth, United Kingdom

Abstract

Biological systems are able to recognise temporal sequences of stimuli or compute in the temporal domain. In this paper we are exploring whether a biophysical model of a pyramidal neuron can detect and learn systematic time delays between the spikes from different input neurons. In particular, we investigate whether it is possible to reinforce pairs of synapses separated by a dendritic propagation time delay corresponding to the arrival time difference of two spikes from two different input neurons. We examine two subthreshold learning approaches where the first relies on the backpropagation of EPSPs (excitatory postsynaptic potentials) and the second on the backpropagation of a somatic action potential, whose production is supported by a *learning-enabling* background current. The first approach does not provide a learning signal that sufficiently differentiates between synapses at different locations, while in the second approach, somatic spikes do not provide a reliable signal distinguishing arrival time differences of the order of the dendritic propagation time. It appears that the firing of pyramidal neurons shows little sensitivity to heterosynaptic spike arrival time differences of several milliseconds. This neuron is therefore

*Corresponding author, Tel.: +357 22892752, Fax: +357 22892701
Email addresses: achilleas.k@cs.ucy.ac.cy (Achilleas Koutsou), g.bugmann@plymouth.ac.uk (Guido Bugmann), cchrist@cs.ucy.ac.cy (Chris Christodoulou)

unlikely to be able to learn to detect such differences.

Keywords: dendritic propagation delays; coincidence detection; membrane noise; synaptic scaling

---

1. Introduction

The detection of sequences of sensory inputs with specific short time delays (e.g., velocity sensitive motion detection or decoding of the firing of Geniculate lagged cells, see Saul, 2008) is a function of biological systems. Sequence detectors are usually modelled as coincidence detectors that exploit appropriate delays of asynchronous individual input to cause a coincidence after the arrival of the last input of the sequence (see for example Branco et al., 2010). Given the adaptability of neural systems, the question arises as to whether learning mechanisms exist that develop appropriate coincidence detectors and then stabilize them during use.

The widely used Spike Timing Dependent Plasticity (STDP) (Markram et al., 1997; Bi and Poo, 1998; Zhang et al., 1998; Froemke and Dan, 2002; Dan and Poo, 2004) learning rule normally requires the postsynaptic neuron to fire a spike and will reinforce all synapses with inputs arriving shortly before that spike. Synapses on distant dendrites whose earlier inputs also contribute to the spike undergo a much weaker reinforcement than proximal dendrites and end up disappearing when resource limitations are considered in the model, as proposed by Letzkus et al. (2006). Branco et al. (2010) have shown that, on the contrary, synapses at various distances from the soma stay strong and contribute to sequence-specific neuronal responses. They did that by activating a succession of synapses by optical uncaging and noted that if the uncaging sequence moves from distal to proximal synapses, the soma showed a higher increase in potential than if the sequence moved away from the soma. Given the results by Branco et al. (2010), it should be possible to reinforce synapses at any distance.

In this paper, we are interested in reinforcing pairs of synapses that are separated by a propagation time delay corresponding to the arrival time differ-

ence of spikes from two different input neurons. We initially examined whether a detector based on dendritic propagation delays in a biophysical model of a pyramidal neuron (Letzkus et al., 2006) can be developed in a bottom-up, unsupervised fashion, i.e., without the soma firing a prior spike to trigger learning on pre-synaptic inputs, following a hypothesis formulated by Bugmann and Christodoulou (2001). A bottom-up approach is in the spirit of experiments conducted by Marom and Shahaf (2002) showing learning without supervisory spiking by the target. The examined mechanism is based on non-linear summation of synaptic EPSPs (Excitatory Postsynaptic Potentials) and their effects, as described for example in Denham and Denham (2001), followed by the backpropagation of the summed EPSP to the dendrites, triggering a learning mechanism at the originating synapse. Simulating this initial approach revealed that the learning mechanism appears to be insufficiently sensitive to differences in time delays. This lead to the development of a second approach using a backpropagating action potential (AP).

In the second approach, a background input current is added to the neuron (at the somatic compartment), to allow the coincidence of pairs of small EPSPs to generate a spike that can then activate learning mechanisms when backpropagating. That background current can be seen as a "learning-enable" signal that is activated when the organism decides that there is a need to learn the current input situation. These processes are designed to allow learning of weights in conditions where they are initially too weak to induce output spikes.

A key element of both approaches is the assumption that inputs from each presynaptic neuron initially target several pre-existing synapses at various positions on the dendrite. These synapses have a probabilistic behaviour and will activate at most one at a time, thus probing various dendritic propagation times (Bugmann and Christodoulou, 2001). The learning rule should then select synaptic pairs separated by the appropriate distance and reinforce them.

This approach differs from the supervised approach used by van Leeuwen (2004) who assumes synaptic relocation along the dendritic tree, or the model by Hüning et al. (1998) that assumes delay modification. The principle of selec-

tion of existing synapses is also used by Gerstner et al. (1998), where the time differences between pre- and postsynaptic spikes determine weight changes, or the work by Eurich et al. (2000) who use a Hebbian learning rule depending on correlations between pre- and postsynaptic activity within a certain time window. Senn et al. (2002) also proposed the use of stochastic synapses, for adapting synaptic delays. Note that the problem treated here is different from that of detecting temporal patterns in a single input spike train, like in Hunzinger et al. (2012), or global oscillations in multiple spike trains like in Kerr et al. (2013). In the context of dendritic delays selection, in this paper we examine the capability of a pyramidal neuron to provide a learning signal selective enough to certain input time differences.

2. Methods

2.1. Overview

Fig. 1 shows a simplified sketch of our model's architecture. Four synapses attach to a neuron's dendrite at increasing distances from the soma. The synapse that is closest to the soma, synapse B, originates from presynaptic neuron B. The rest of the synapses, A1, A2 and A3, originate from presynaptic neuron A.

Presynaptic neurons A and B fire the same spike trains with a fixed time delay, Δt. In other words, whenever neuron A fires at a time t, B fires at $t + \Delta t$. In this paper, we aim at reinforcing synapse A2. We consider two scenarios (Fig. 1):

(i) An EPSP from A2 arrives at B after Δt time, thus coinciding with the time the EPSP at B is created. The coinciding EPSPs are amplified, creating an increase in postsynaptic potential at B, which travels back to the A synapses.

(ii) The EPSPs from A2 and B coincide at their arrival at the soma and trigger a somatic spike, creating a back-propagating action potential which travels back to the synapses.

In both cases, the back-propagating potential is expected to cause weight changes in the active synapses (i.e., the synapses that have recently been active).

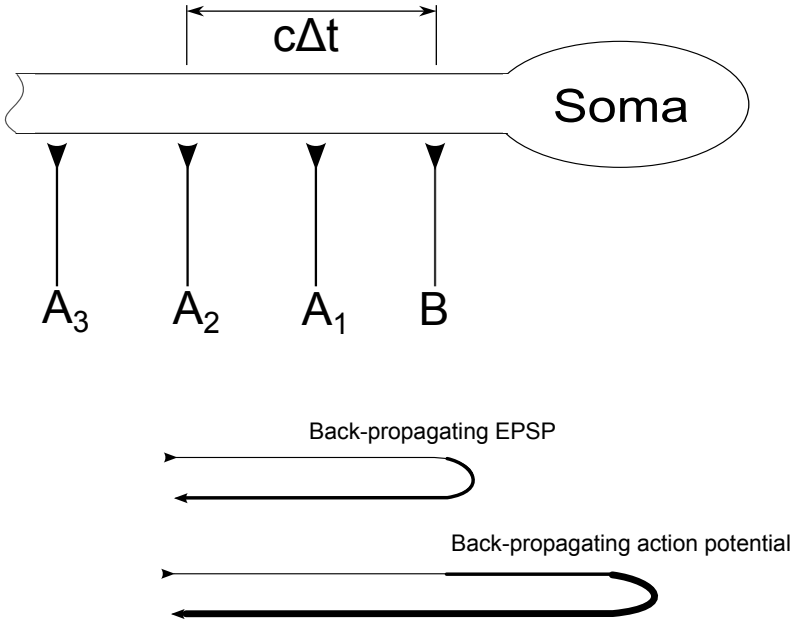

Figure 1: Schematic of our model's architecture consisting of a simple neuron with 4 synapses. B is a proximal synapse, while synapses A1–3 are at increasing distances from the soma. All A-synapses originate from the same pre-synaptic neuron (neuron A) and B originates from a different one (neuron B). See the text for an explanation of the two back-propagation diagrams.

The purpose of both scenarios is to make the post-synaptic neuron sensitive to the firing delay between pre-synaptic neurons A and B, by reinforcing only synapse B and the corresponding A-synapse whose distance from B is such that the EPSP from A coincides with the EPSP from B, at location B. In other words, if c is the propagation speed and Δt is the firing delay between pre-synaptic neurons A and B, the learning mechanism should reinforce an A-synapse that is at a distance $c\Delta t$ from synapse B. In all our scenarios, the A-synapse that is located at the ideal distance from B will be labelled A2. Our methods require that synapses are stochastic with a low probability of release

(Pun et al., 1986; Redman, 1990; Senn et al., 2002), since synapses A1, A2 and A3 all originate from the same pre-synaptic neuron, but should receive individual reinforcement. By setting the release probability sufficiently low, we can consider that the probability of having two or more A-synapses active at the same time is negligible.

The main difference between the two approaches is the lack of somatic spiking in the first approach. The first scenario relies on the amplification and backpropagation of a potential, caused by the coinciding EPSPs at the dendritic location of synapse B. Plasticity, in this scenario, would occur as a result of the changes caused along the dendrite by the backpropagating amplified EPSP, in the absence of somatic spiking. The second scenario follows a more traditional approach to learning, where the coinciding EPSPs trigger a somatic action potential that is able to cause synaptic changes based on a STDP-type learning rule.

2.2. Model

For our simulated experiments, we used the NEURON simulation environment (Hines and Carnevale, 1997) using a reconstructed layer 5 pyramidal neuron model, originally built by Stuart and Spruston (1998). This model was modified by Letzkus et al. (2006)[1] to account for active properties, by including voltage-gated ion channels at the following densities (in $\mathrm{pS\,\mu m^{-2}}$):

- Soma: $g_{Na} = 3000$, $g_{Kv} = 30$, $g_{Ka} = 0.06$, $g_{Kca} = 2.5$, $g_{Km} = 2.2$, $g_{CaT} = 0.0003$.
- Dendrites: $g_{Na} = 40$, $g_{Kv} = 30$, $g_{Ka} = 0.03$, $g_{Kca} = 2.5$, $g_{Km} = 0.05$, $g_{CaT} = 0.0003$.
- Distal dendrites ($> 600\,\mu\mathrm{m}$ from the soma): $g_{Na} = 40$, $g_{Kv} = 30$, $g_{Ka} =$

[1]The biophysical pyramidal neuron model is available at `https://senselab.med.yale.edu/ModelDB/ShowModel.cshtml?model=108459`

0.03, $g_{Kca} = 2.5$, $g_{Km} = 0.05$, $g_{CaT} = 0.001$, $g_{Ca} = 1.25$ (slow high-voltage activated calcium).

- Axon: $g_{Na} = 30\,000$, $g_{Kv} = 400$.

This model, in principle, is able to generate dendritic calcium spikes, however these are not produced in the scenarios simulated in this paper. The specific membrane resistance was $15\,\mathrm{k\Omega\,cm^2}$, the membrane capacitance was $1\,\mu\mathrm{F\,cm^{-2}}$ (15 ms time constant), the axial resistance was $125\,\Omega\,\mathrm{cm}$. Somatic resting potential, in the absence of any background current, was $-79\,\mathrm{mV}$ and the AP threshold was $-63\,\mathrm{mV}$. We further modified the resulting model by Letzkus with the addition of synaptic locations and their weights.

Synapses were placed along the main branch of the dendrite at increasing distances, as shown in Fig. 2. Excitatory postsynaptic currents (EPSCs) produced due to AMPA (α-amino-3-hydroxy-5-methyl-4-isoxazolepropionic acid) receptors were modelled as double exponentials with a rise time $\tau_{rise} = 0.2\,\mathrm{ms}$, a decay time $\tau_{decay} = 2\,\mathrm{ms}$ and a maximum amplitude (the *weight* of the synapse). Each synapse also contained NMDA (N-methyl-D-aspartate) receptors, with a NMDA-AMPA ratio of 0.2, as in Letzkus et al. (2006). The NMDA component was simulated with a kinetic model, developed and described in Kampa et al. (2004), and was part of the model taken from Letzkus et al. (2006). The NMDA receptor was modelled by a 10-state Markov model, which was constructed by adjusting the reaction rates to fit experimentally recorded data. This resulted in apparent decay times on the order of 50–60 ms, where the larger values occur at more distal synapses. During our simulations, potentials were recorded in the dendritic compartment behind each synapse as well as at the soma.

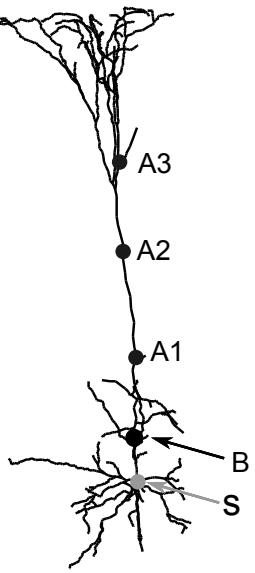

Figure 2: Synaptic locations on a morphological reconstructed neuron model. The grey location, indicated by S is the location of the soma.

2.3. Scaling

As mentioned in Section 1, our second approach relies on a constant background current that raises the resting potential of the neuron, such that two coinciding EPSPs would trigger an action potential at the soma, but a single EPSP should not. The current is applied directly to the somatic compartment of the model. These requirements define a range of background current amplitudes (0.22–0.24 nA) and we use this range to explore the behaviour of the neuron. For each value of the current amplitude, a different set of synaptic weights is required. The effect of the current amplitude on the results is discussed in Section 3.2.5. The figures shown in this section illustrate the behaviour for an example case of 0.222 nA constant background current, which raises the effective resting potential to -72.5 mV (6.5 mV higher than the default rest).

Synaptic weights were scaled such that an EPSP from any of the synapses had the same peak depolarisation level at the soma. The reason for the uniform scaling of synaptic weights was to make the effective difference at the

soma between specific pairs of EPSPs depend only on the propagation delay of the potential and the input spike time difference. This reflects the results of Häusser (2001) showing that the amplitude of the EPSP arriving at the soma is independent of the distance of the originating synapse.

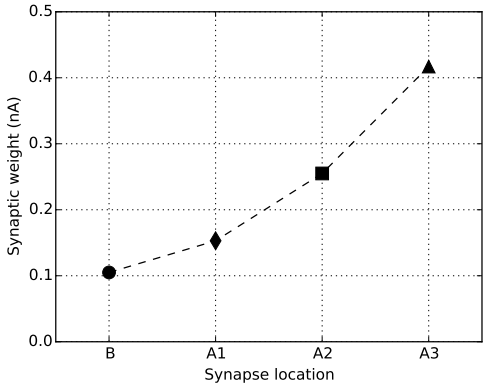

Figure 3: Example of synaptic weights after scaling. Weights (excitatory postsynaptic peak currents) were scaled to produce a depolarisation of 1 mV at the soma when a constant background current is applied with an amplitude of 0.222 nA. The symbols used to represent each point will be used throughout the paper to reference each synaptic location: B ●, A1 ⧫, A2 ■, A3 ▲.

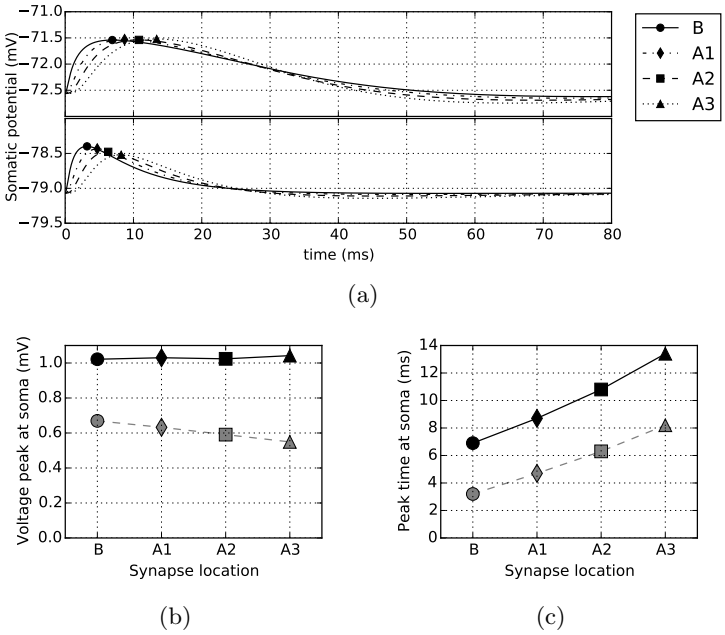

Figure 4: (a) Depolarisation at soma for EPSPs evoked at each synaptic location with a constant background current of 0.222 nA (top) and without (bottom). (b) Peak potential at the soma with background current (black, solid line) and without (grey, dashed line). The peak is measured as the difference between the maximum potential reached when the EPSP is evoked and the *effective* resting potential (i.e., the resting potential immediately before the EPSP is triggered). (c) Time to peak (peak time minus onset of EPSP) at the soma with background current (black, solid line) and without (grey, dashed line). In all figures, the symbols correspond to a synaptic location: B ●, A1 ♦, A2 ■, A3 ▲.

Fig. 3 shows the weight of each synapse after the calibration was complete. The effects of the background current on the scaled weights can be seen in Fig. 4. Fig. 4a shows the potential recorded at the soma for four EPSPs, evoked separately at each of the synaptic locations with a constant background current applied (top) or not applied (bottom). Fig. 4b shows the peak depolarisation caused at the soma by an EPSP from each synapse, with (top line) and without (bottom line) the background current applied. These values are calculated by subtracting the effective resting potential, i.e., the membrane potential immediately before the EPSP is triggered, from the peak potential reached during

the EPSP. Fig. 4c shows the time when the peak potential was reached, both with (top line) and without (bottom line) the background current applied. The results show that adding a background current has three effects on the EPSPs:

- It shifts the voltage upwards, as expected, but also increases the depolarisation caused by an EPSP. This effect becomes a little stronger with greater distance from the soma (Fig. 4b).
- It increases the time required for the EPSP to reach its peak at the soma (Fig. 4c).
- It also affects the shape of the EPSPs arriving at the soma, with the expected widening with distance largely being eliminated (in Fig. 4a, top curve, the width at 95 % of the height is for B: 7.1 ms, A1: 7.1 ms, A2: 7.1 ms and A3: 7.3 ms). Note that, without background current, EPSP peaks are narrower and show the usual distance dependence (in Fig. 4a, lower curve, the width at 95 % of the height is for B: 2.4 ms, A1: 2.8 ms, A2: 3.2 ms and A3: 3.6 ms).

These effects have also been observed in *in vitro* studies on cortical and hippocampal pyramidal cells (Deisz et al., 1991; Stuart and Sakmann, 1995; Fricker and Miles, 2000; González-Burgos and Barrionuevo, 2001; Zsiros and Hestrin, 2005). Fricker and Miles (2000) suggest that when the membrane potential is depolarised, the activation of inward currents tends to increase the amplitude of EPSPs and prolongs their decay.

2.4. Simulation procedure

Only two synapses were considered in each simulation. The assumption in our model is that synapses are probabilistic with low activation probability and we examine the cases where at most only one of the A-synapses is active at a time, along with B. Therefore, activation of synapses was induced in pairs, one of the A synapses and the B synapse, with a delay Δt, in order to examine the AP firing behaviour for separate instances of stimulus arrival. The simulation was

run for 1 s before evoking any EPSPs at the synapses, to allow the potential to stabilise from initial conditions. This was especially required in the case where background current was applied. The background current is always applied directly to the somatic compartment of the neuron.

3. Results

3.1. Approach 1: Backpropagating coincident EPSPs

In this section we report on a simulation of the forward propagation of an EPSP from A2, its coincidence with an EPSP generated by an input at B and then the backpropagation of the resulting coincident EPSP to A2. In order to evaluate the expected degree of reinforcement of synapse A_i, we calculate the integral of the NMDA conductance at that synaptic location, as in Letzkus et al. (2006). Fig. 5 shows the integral of the NMDA conductance (normalised to the maximum) across a range of input delays (Δt) after a pair of input spikes activated a pair of synapses. For each simulation, one A-synapse was activated followed by an activation of synapse B after a delay of Δt. The order of synapse activation was reversed (B A) for negative Δt. The NMDA conductance was recorded at the location of the A-synapse being activated and the integral over the entire simulation time was calculated (see Fig. 5).

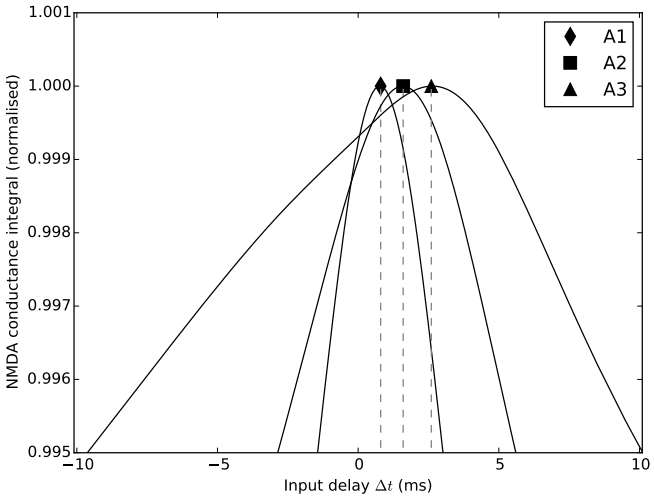

Figure 5: Integral of the NMDA conductance during the activation of a pair of synapses, (A_i B). The conductance was recorded at the location of the A-synapse (A_i) in each case. The symbols at the peak of each curve represent the three synaptic locations, A1, A2 and A3 respectively. No background current was added in this scenario.

Table 1: Normalised integral of the NMDA conductance for specific input delays Δt. Each value is the delay which maximises the integral at one of the three locations, 0.8 ms for A1, 1.6 ms for A2, and 2.6 ms for A3.

	Δt		
	0.8 ms	1.6 ms	2.6 ms
A1	1.0000	0.9997	0.9997
A2	0.9997	1.0000	0.9999
A3	0.9997	0.9996	1.0000

As Fig. 5 shows, the integrated NMDA conductance for each synapse peaks at different delays, corresponding to the dendritic propagation times from each A-synapse to B. However, the difference in conductance integrals between synapses,

for a given time delay, are very small. For instance, when the input delay is such that it maximises the integral at A2, i.e., $\Delta t = 1.6\,\text{ms}$, spike pairs (A1 B) and (A3 B) have normalised NMDA conductance integrals of 0.9997 and 0.9996 respectively (see Table 1). A learning rule which is based on the integral of the NMDA conductance, as in Letzkus et al. (2006) (see their supplementary Fig. 5[2]), would apply reinforcements with minute differences between synapses, for delays -1–$3\,\text{ms}$. This can be seen in Fig. 5, where all curves are above 0.995 within the aforementioned range of delays. Ideally, in order for the neuron to learn to respond to a specific spike delay which corresponds to the propagation delay between A2 and B ($\Delta t = 1.6\,\text{ms}$), the reinforcement at that delay should be significantly different for each synapse, such that A2 receives a significantly stronger reinforcement when activated compared to A1 or A3. Our results show that this is not the case. Backpropagating coincident EPSPs are therefore unlikely to provide sufficiently strong differentiating signals.

Given this result, we have investigated a different approach using backpropagating action potentials instead of EPSPs. This is the topic of the next section.

3.2. Approach 2: Backpropagating Action Potential

Here we examine the idea that, by adding a background input current to the neuron, the two small coincident EPSPs become able to cause a spike that then triggers learning mechanisms when backpropagating to the recently active synapses. As learning by backpropagating APs is well documented, the main issue dealt with in this section is the appropriate generation of that action potential. Again, we focus on learning at synapse A2, ignoring B.

Fig. 6 shows two ways in which action potential generation is affected by the application of a constant background current to the soma. Fig. 6a shows how the width of the *firing domain* grows with increased background current. Each pair of curves show the minimum and maximum input delays (the delay

[2]Supplementary Fig. 5 is available at `http://www.jneurosci.org/content/suppl/2006/10/11/26.41.10420.DC1/LetzkusSuppl.5comp.gif`

between activation of an A-synapse and synapse B) that trigger a somatic spike across a range of background current amplitudes, for each synaptic pair (A_i B). Background currents below 0.22 nA do not raise the effective resting potential high enough to enable a somatic spike, even when EPSPs coincide perfectly at the soma. Background currents above 0.227 nA, which would drive the spike domain outside the range −20–20 ms, were not considered. Fig. 6b shows the effect of increasing the background current on the somatic spike delay (the time of the somatic spike minus the time of the second EPSP's onset). For each synaptic pair (A_i B), we used an input delay which corresponds to the difference in peak times at the soma (as seen in Fig. 4c).

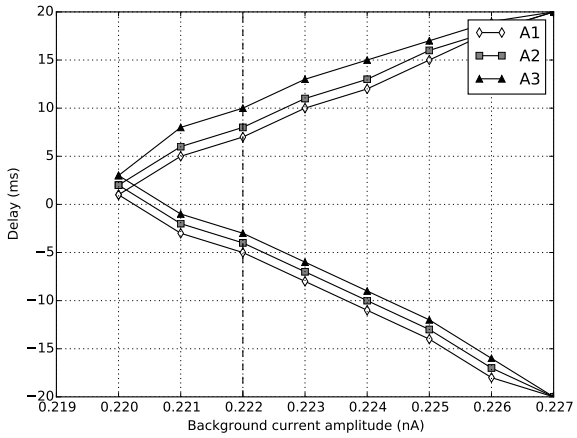

(a)

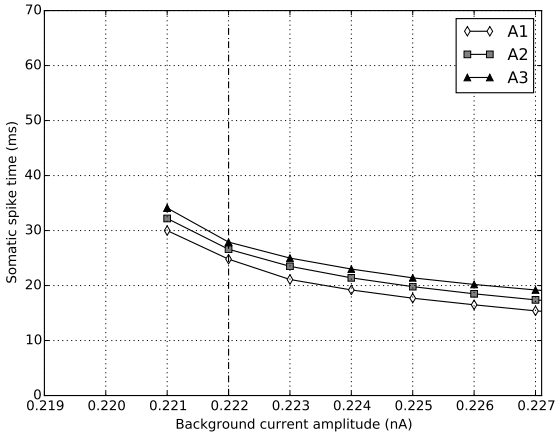

(b)

Figure 6: (a) Effect of the background current amplitude on the range of input delays that cause a response. Input delays outside the range −20–20 ms were not considered. (b) Effect of the background current amplitude on the somatic spike time for (A_i B) spike pairs. For each pair, the input delay which corresponds to the internal propagation delay was used (A1: 1.8 ms, A2: 3.8 ms, A3: 6.5 ms). The dashed vertical line in both figures indicates the background current amplitude of 0.222 nA used as an example throughout this paper. The number of samples on both figures have been decimated for clarity.

3.2.1. Relative timing conditions for action potential generation

To measure the selectivity of the coincidence detection mechanisms, we ran simulations where we varied the time delay between spike arrival time at an A-synapse and synapse B. In the example shown in Fig. 7 (background current with amplitude 0.222 nA), the neuron fires for a range of time delays, and cannot discriminate, in a binary way (which is by firing or not firing) time differences shorter than around ± 7 ms. The domain of firing rises towards more positive delays for more distant synapses, showing the effect of an increasing dendritic propagation time. The rise and width of the firing domain are explained in Section 3.2.3.

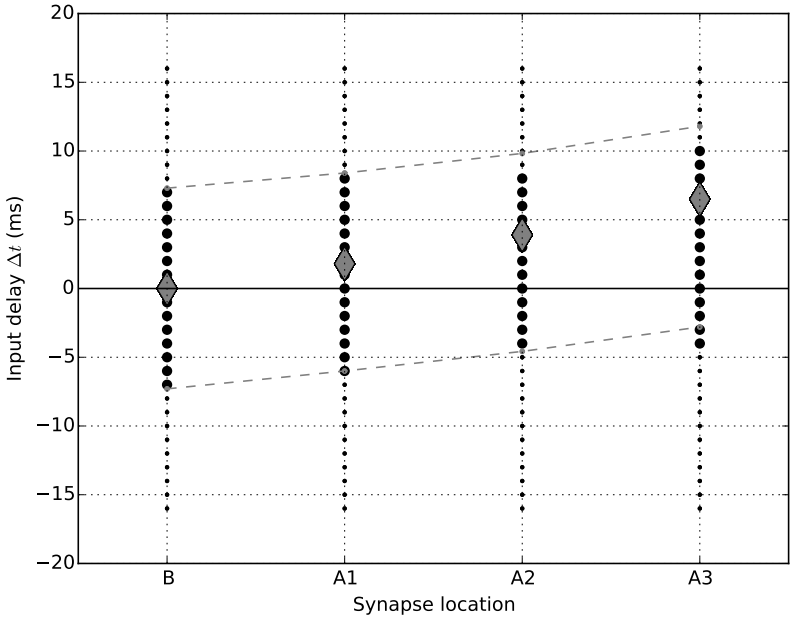

Figure 7: Spike occurrence for the indicated combinations of input delay (Δt) and synapse location for an example case with background current amplitude of 0.222 nA. The bigger dots denote cases where a spike was fired, while the smaller ones show cases where no somatic spike occurred. Negative delays denote cases where the B synapse triggered an EPSP before the A-synapse. The leftmost column of dots represents simulations where both EPSPs were triggered at the B synapse. The dashed grey lines correspond to the maximum and minimum delays that cause a somatic AP according to the model described in Section 3.2.3. The diamond shaped points on each column represent the optimal delay between each synapse and synapse B for maximum depolarisation, which is the difference in peak times at the soma between an A-synapse and synapse B (d_{A_iB}, third column of Table 2).

3.2.2. Action potential timing

Fig. 8a shows the time of AP production relative to the input time. The somatic spike delay (d_S) was calculated as the somatic spike time (t_S) minus the initiation time of the second input spike, $d_S = t_S - \max(t_A, t_B)$, where t_A and t_B are the times of EPSP initiation from pre-synaptic neurons A and B respectively. The amplitude of the background current in all cases was 0.222 nA.

On the right-hand side of the horizontal axis (which shows the input delay),

positive delays indicate that synapse B receives the last input. On the left-hand side, synapse A receives the last input. The four curves show a lateral shift by a time slightly shorter than the difference between the time-to-peak (T_p) delays of each individual EPSP (Fig. 4). The lateral shift shows clearly that the dendritic propagation time affects the response to inputs with different time difference. However, it also shows a very flat minimum that provides little differentiation between time differences close to the difference in T_p between synapses. All AP production times occur at least 22 ms after the arrival of the last of the two inputs, due to the integration of long lasting NMDA currents needed to cause firing. They take around 2–3 ms to propagate back to an A-synapse, giving a round-trip time of 24 ms or more.

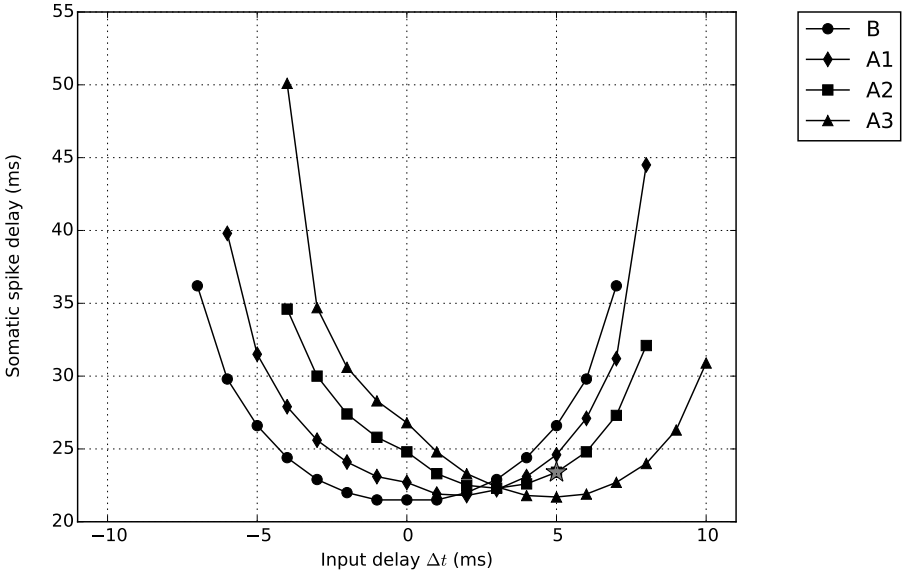

(a)

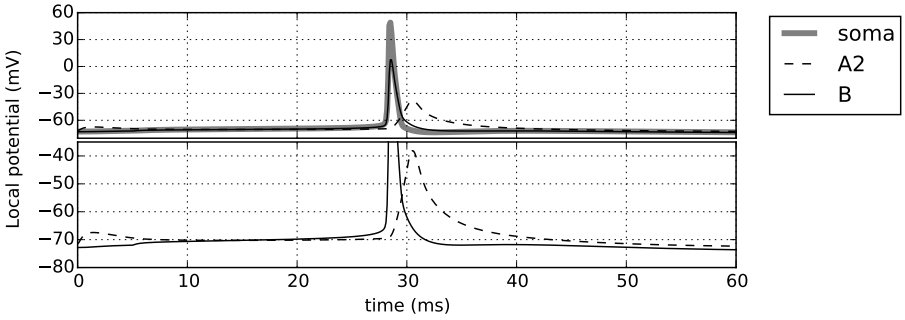

(b)

Figure 8: (a) Action potential production time after the last input spike for the indicated synapses and for different delays between spike input at B and A. Positive delays correspond to the B input occurring after the A input. The range of delays correspond to the ones in Fig. 7. (b) Example voltage traces for a single simulation where an action potential was generated. The case shown corresponds to the point in subfigure (a) marked by the grey asterisk (synapse A2, $\Delta t = 5\,\mathrm{ms}$). The top panel shows the voltage at all three locations, A2, B and soma. The bottom panel shows the depolarisation at dendritic locations B and A2 in an expanded ordinate, for clarity. In subfigure (b), the time of the input at synapse B corresponds to time 0. Both subfigures are sample cases with background current set at $0.222\,\mathrm{nA}$.

3.2.3. Modelling the selectivity

Fig. 7 shows that an AP is generated for a range of time differences of input spikes. To explain the upper and lower boundaries of the domains of firing, we have formulated a simple model. The EPSPs arriving at the soma from B and from A_i ($i = 1, 2, 3$) cause a maximal potential increase when their peaks are coincident. This occurs when the delay (d_{A_iB}) between input spikes matches the difference in arrival times (differences in time to peak) at the soma:

$$d_{A_iB} = T_{p_{A_i}} - T_{p_B} \tag{1}$$

where $T_{p_{A_i}}$ and T_{p_B} are the times to peak for respectively inputs from A_i and B. When both inputs arrive at B, the delay is zero ($d_{BB} = 0$).

Now, let us assume that an exact coincidence is not needed and that the peaks are efficient over a given time window. A simple way to estimate this is to measure the duration T_w of the width of the EPSP peak at, say, 95 % of its maximum height. The results are shown in Table 2. All the peaks have a width of about 7 ms. So, the inputs can be desynchronized by ± 7 ms and still produce APs. More precisely, the maximum delay $\Delta t_{\max}$ and minimum delays $\Delta t_{\min}$ are given by:

$$\Delta t_{\max} = d_{A_iB} + 0.5T_{w_A} + 0.5T_{w_B} \tag{2}$$

$$\Delta t_{\min} = d_{A_iB} - 0.5T_{w_A} - 0.5T_{w_B} \tag{3}$$

It turns out that this simple model explains the behaviour of the domain of firing times in Fig. 7 (dashed lines). To obtain the correct slope of the curves, we had to replace the delay calculated from Eq. (1) with the actual best delay given by data in Fig. 8a (see Table 2).

Table 2: Model data and results. The results $\Delta t_{\max}$ and $\Delta t_{\min}$ are shown in Fig. 7. T_p is the time-to-peak, i.e., the time when the EPSP reaches maximum depolarisation at the soma. $d_{A_i B}$ is the difference between the two peak times from A_i and B respectively. This value is 0 when both EPSPs are triggered at B. T_w is the *peak duration*, which is measured as the duration where an EPSP is above 95 % of its maximum height. $\Delta t_{\max}$ and $\Delta t_{\min}$ are the calculated maximum and minimum delays that cause a somatic AP for an EPSP coming from a given synapse, while coupled with an EPSP from B. All values in the table are in milliseconds.

Synapse	T_p	$d_{A_i B}$	Delay from Fig. 8a	T_w	$\Delta t_{\max}$	$\Delta t_{\min}$
B	6.9	0	0	7.1	7.3	−7.3
A1	8.7	1.8	1.12	7.1	8.48	−5.92
A2	10.8	3.9	2.8	7.1	10	−4.4
A3	13.4	6.5	4.8	7.3	12.1	−2.5

3.2.4. Achieving the required selectivity with constant background current

In order to reinforce only one of the A-synapses (A2), the input pair (A2 B) should cause a somatic spike, while the other pairs (A1 B) and (A3 B) should not. This requires the maximum input delay $\Delta t_{\max}$ for A2 to be smaller than the $\Delta t_{\min}$ for A3, and for the minimum delay $\Delta t_{\min}$ for A2 to be larger than the $\Delta t_{\max}$ for A1. Intuitively, this can be understood as a shrinking of the domain between the two dotted lines in Fig. 7 until there is no overlap between the delay domain of different input synapses (i.e., the columns of dots are horizontally separable). This results in a very narrow domain of operation due to the shallow slopes of the max and min model curves in Fig. 7. Given the difference between d_{A3B} and d_{A1B} (taken from Fig. 8a and Table 2), the firing domain at A2 cannot be wider than ± 0.92 ms. This can be achieved with currents very close to the firing threshold, i.e., currents only slightly above 0.22 nA (see Fig. 6a). Given that the half range Δt of delays between an input at B and an input at A2 for

which the neuron fires (Fig. 6a) can be approximated by:

$$\Delta t(I) = \frac{15.5\,[\mathrm{ms}]}{0.006\,[\mathrm{nA}]}(I\text{–}0.22\,[\mathrm{nA}]) \tag{4}$$

we can calculate the maximum background current for which $\Delta t \leq 0.92\,\mathrm{ms}$. Eq. (4) is only valid for currents above 0.22 nA and no firing takes place below that current. The current that achieves this value is 0.220 178 nA which is approximately 0.2 pA above the threshold current. Such precision is practically impossible to achieve. In addition, the membrane voltage is actually noisy.

3.2.5. Effect of level of noisy background current on selectivity

We will examine hereafter the effect of the lowest possible membrane noise on the selectivity. According to Destexhe and Paré (1999), the smallest observed voltage fluctuations have a standard deviation of around 0.4 mV, with a voltage range of 0–2.5 mV. At this low level of noise, their data (see in Fig. 2b of their paper) shows that the membrane potential does not have a Gaussian distribution. We found that a better fit is obtained with a Beta distribution shown in Fig. 9a and described by Eq. (5).

$$B(V) = C\left(\frac{V}{2.5}\right)^{\alpha-1}\left(1-\frac{V}{2.5}\right)^{\beta-1} \tag{5}$$

where $C = 22.4$ is a normalisation constant ensuring that the integral of $B(V)$ is equal to 1 between $V = 0$ and $V = 2.5\,\mathrm{mV}$.

To fit the data in Destexhe and Paré (1999) we set the parameters of Eq. (5) to $\alpha = 2$ and $\beta = 7$, which results in a maximum fluctuation of 2.5 mV and yields a standard deviation of 0.4 mV and a peak at 0.5 mV, both matching experimental values. In order to relate data on potential fluctuations to results of our simulations, we calculated the equivalent background current I for each potential using the locally (around 0.22 nA) linear relation found in our simulations (figure not shown):

$$V(I) = -72.66\,[\mathrm{mV}] + 55\,[\mathrm{mV/nA}]I \tag{6}$$

For each current we then calculate the time window for firing using Eq. (4) that is based on Fig. 6a for inputs at the A2 synapse. To calculate the value of the

average half time window we consider the distribution of membrane potentials above threshold. In our case, the threshold is defined by an equivalent current of 0.22 nA. Consequently, the average half time window can be expressed as:

$$\overline{\Delta t} = \frac{\int_{V_0}^{V_0+2.5\,\mathrm{mV}} \Delta t(I(V))B(V)S(I(V))dV}{\int_{V_0}^{V_0+2.5\,\mathrm{mV}} B(V)S(I(V))dV} \tag{7}$$

where $S(I)$ is either 1 or 0, reflecting whether the neuron can fire a somatic spike at the voltage V or not. The denominator is a normalisation term representing the fraction of cases where the voltage is above the minimum needed to fire. Note that experimental data in low noise conditions show fluctuations of the membrane potential reflecting excitatory inputs by fast (15–30 ms) potential rise, followed by a slower (200–300 ms) decay to the average potential (estimated from Fig. 2 in Destexhe and Paré, 1999). We can therefore assume, as a first approximation, that the potential stays constant long enough for the duration of one (A_i B) input sequence and the summation of the two EPSCs at the soma.

To explore the effects of noise on the selectivity (measured by the average time window of firing, Eq. (7)) of the neuron, we vary the baseline of the background current amplitude and assume fluctuations of the membrane potential as described above. From Eq. (6) we find that a background current increase of 0.045 nA is needed to increase the somatic membrane voltage by 2.5 mV. We then examine three cases:

(i) The fluctuating current is always above threshold (0.22–0.265 nA).

(ii) The fluctuating current is partly below and partly above threshold (0.20–0.245 nA).

(iii) The fluctuating current is almost always below threshold with only a small part of the tail of the distribution above threshold (0.177–0.222 nA).

The results are as follows: In case (i), the potential (input current) is always sufficient to cause a spike if the time interval between input spikes is right (input current $\geq$ 0.22 nA). The average time window between inputs to A and B (Eq. (7)) can be up to $\pm$30 ms away from the ideal time difference (the propagation time difference between the A_i and B synapse, d_{A_iB}). In case (ii),

the membrane potential is often (93 % of the time) below the threshold when even inputs with the perfect time interval are not able to cause firing. In the remaining 7 % of cases, where the current is above 0.22 nA, the average time window is still quite high, with ±10 ms. In case (iii), I_0 is small enough to achieve the ideal time window of ±0.92 ms, but the neuron is responsive only in 2×10^{-8} of cases, which is very close to never. The image that emerges is that generating appropriately selective somatic spikes as a learning signal is almost impossible.

3.2.6. Effect of level of noisy background current on frequency of learning feedback

We have also examined whether the probability of firing a somatic spike (that triggers learning) is different enough between pairs of synapses. Ideally, the firing probability of the neuron when (A2 B) are activated should be significantly higher than when (A1 B) and (A3 B) are activated with the same input delay Δt, for a given level of baseline background current. Assuming a noisy background current, as in Section 3.2.5, with a baseline amplitude of less than 0.22 nA, the probability of somatic firing, even when inputs coincide perfectly at the soma, is less than 1. The firing probability depends on the Beta distribution seen in Fig. 9a. The synaptic location and Δt together define the minimum background current amplitude required to fire a somatic spike, which we denote with $I_{th}(A_i, \Delta t)$. We can determine these values from the data shown in Fig. 6a.

We investigate the case where $\Delta t = 2$ ms since, for that input delay, the pair (A2 B) will cause a somatic response when the background current amplitude is $I_{th}(A2, 2\,\text{ms}) = 0.22\,\text{nA}$, while $I_{th}(A1, 2\,\text{ms}) = I_{th}(A3, 2\,\text{ms}) = 0.2205\,\text{nA}$. We examine whether this difference in minimum current amplitudes results in a substantial difference in firing probabilities between the three synaptic pairs, for different values of baseline current amplitude, I_0.

Fig. 9b shows the probability of firing of all three pairs, for input delay $\Delta t = 2$ ms, across the full range of baseline input currents I_0 that have a firing probability ≤ 1. The noisy current causes fluctuations of the membrane voltage

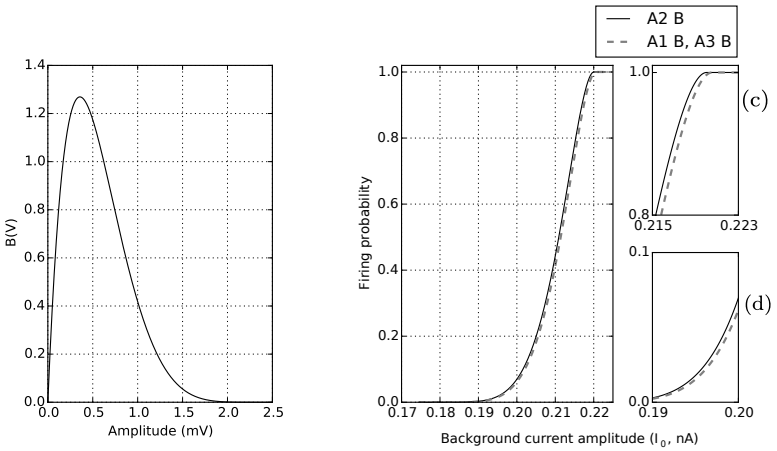

Figure 9: (a) Beta distribution of membrane potential amplitudes that fit the experimental data from Destexhe and Paré (1999) (Fig. 2a). It represents the potential above *effective* rest, where the effective rest is the minimum (baseline) resting potential of the membrane when the neuron is injected with a fluctuating current. (b) Firing probability of the neuron as a function of the baseline injected background current, I_0. The probabilities are calculated using Eq. (7). The smaller figures on the right hand side show the upper (c) and lower (d) parts of the probability curves at different scale to emphasize the small difference between the two curves. In order to calculate the firing probability of (A1 B) and (A3 B), we set the minimum current required for firing to 0.2205 nA, instead of 0.22 nA, which is the minimum current required for firing for those synaptic pairs when the input delay is $\Delta t = 2$ ms (seen in Fig. 6a). The dashed line on the figure represents the firing probability for both (A1 B) and (A3 B), since both synaptic pairs have the same current threshold.

up to 2.5 mV corresponding to current fluctuations up to 0.045 nA. Therefore, the lowest baseline input current I_0 that has a non-zero probability of causing a spike is $I_{th}(A2, 2\,\text{ms}) - 0.045\,\text{nA} = 0.175\,\text{nA}$.

The curves in Fig. 9b show that the difference in firing probabilities is very small for the full range of background current amplitudes. Is this difference too small to cause significantly higher reinforcement of A2 compared to A1 or A3? To address this, we investigated whether the relative differences in firing probabilities were large for high firing rates or for low firing rates. More specifically, we have examined two cases, one near the top (Fig. 9c) and one near the bottom of the firing probability curve (Fig. 9d). For these cases:

(i) The background current fluctuates between 0.195 nA and 0.24 nA.

(ii) The background current fluctuates between 0.220 nA and 0.265 nA.

The first case represents a range of current (and by extension voltage) fluctuations which have a very small probability of causing a spike while the second case represents a current range which has a very high probability of causing a spike.

In case (i) the probability of firing is 0.018 for (A2 B) and 0.015 for (A1 B) and (A3 B). This means that (A2 B) triggers 20 % more spikes than the other two pairs. However, the frequency of learning signals is very low, with only 18 spikes generated for 1000 input pairs from (A2 B). A higher difference in firing probabilities could be obtained but at the cost of even lower firing frequencies.

In case (ii), the inverse problem occurs. The probability of firing is 1 for (A2 B) and 0.996 for (A1 B) and (A3 B). In this case, many spikes are produced, but the difference between firing probabilities is very small (0.4 %).

Overall, either we have many somatic spikes with little differentiation between input pairs (0.4 %) or, in the case where there is some differentiation (e.g., 20 % or more), learning is possibly impractically slow.

4. Discussion

The aim of this work was to examine whether it is possible to train a neuron to detect input spikes from different sources with specific delays. All mechanisms considered attempted to exploit dendritic propagation times between pairs of synapses. The paper has focused on the possibility to generate appropriate training signals to reinforce pairs of synapses with internal propagation time matching the external spike arrival time difference.

In the first approach, using backpropagating EPSPs, we found that even in the best case, where the peak of an EPSP from A2 coincided perfectly with the peak of an EPSP at B, the difference in integrated NMDA conductance was too small to be of practical use. Thus, the use of a non-spiking approach as suggested in Bugmann and Christodoulou (2001) is not effective in a pyramidal neuron.

In the second approach, we generated a somatic action potential in response to the coincidence of EPSPs from synapses A and synapse B. Unfortunately, our work has revealed two problems:

(1) Although in the case of a noiseless constant background current at its minimum of 0.22 nA, the time window for firing is encouragingly smaller than the desired ± 0.92 ms, when minimal noise is considered, as observed by Destexhe and Paré (1999), reveals that the practical time window is closer to ± 10 ms. Triggering a spike only when the input time delay matches the propagation time delay of a specific synaptic pair is therefore impossible. (2) We then examined whether the probabilities of producing an AP were sufficiently different between synapse pairs (A1 B), (A2 B) and (A3 B). We found that either (i) there is a difference but with a very low probability of an AP being produced, or (ii) many APs are produced but their firing probability does not differentiate between synaptic pairs.

We also observed that there is a variation of the firing time of the APs, depending on the difference between ideal input time difference and the actual one. In Fig. 8a, this difference is at most around 10 % for large input time

differences, but around values relevant to distinguishing between A1, A2 and A3, the curves show little sensitivity to be exploited, for instance, in a STDP-type learning rule. Furthermore, in the presence of noise, it is unlikely that these somatic AP delays remain reliable indicators of input time delays.

Thus, there appears to be no usable signal to reinforce one A-synapse against all the others. Although pyramidal neurons in the brain vary in electrical properties, e.g., with membrane time constants ranging from 9–60 ms (15 ms in the model used in this paper), they share sufficient common structural properties (Spruston, 2008) for these results to be of a general validity.

The selectivity of the neuron can be measured by the height of the row of dots in Fig. 7. Our example for a background current of 0.222 nA shows that APs are generated for delays between the two input spikes varying typically by ± 7 ms for any pair of synapses. Our computational model proposes that the selectivity is related to the width of the EPSP arriving at the soma (where width refers to some effective top part of the EPSP profile, estimated at around 95 % of the height in our example). Even synapses attached directly to the soma show a width of around ± 7 ms. One may ask if this is also the time window for coincidence detection? Without background current, EPSPs arriving at the soma have much narrower peaks, around 3 ms *vs* 7 ms in our example (Table 2). However, our simulations show that, when the potential rises toward the firing threshold, EPSPs become wider. This raises the question of whether a number of superposed narrow EPSPs actually stay narrow. This may be addressed in further studies.

5. Conclusions

Our results suggest that it is not possible for a pyramidal neuron to learn to distinguish time delays of the order of dendritic propagation time between synapses. Our study of a biophysical model of a pyramidal neuron considered multiple learning mechanisms and various features of the behaviour of the neuron which could, in principle, give rise to signals that can distinguish between

different input time delays.

Firstly, a learning mechanism which relies on the changes in NMDA conductance at the synaptic site, in the presence of coincident inputs and in the absence of somatic spiking (Approach 1), was shown to be insufficient for producing a learning signal that is significantly higher for the coincident synaptic pair, when compared to other synaptic pairs.

Secondly, methods relying on a somatic spike being generated also failed to provide a mechanism for learning temporal delays. In the presence of somatic spiking (Approach 2), we examined:

(i) the range of input time delays, at each synaptic pair, which produce a somatic response spike (we refer to this as the *firing domain*, Sections 3.2.1 and 3.2.3);

(ii) the timing of the action potential, relative to the input, for the full range of input time delays (Section 3.2.2);

(iii) the effect of background current noise on the width of the *firing domain* of each synaptic pair (Section 3.2.5);

(iv) the effect of background current noise on the firing frequency (or firing probability) of the neuron for inputs from different synaptic pairs (Section 3.2.6).

None of these features provided a strong differentiating signal for different input synapses. More specifically:

(i) The *firing domain* is not sufficiently distinct between synapses (i.e., the domains always overlap);

(ii) Action potentials are generated with delays that do not vary significantly when triggered by different synapses, in the range of input delays considered by our study.

(iii) In the presence of noise, the average background current can be reduced to the point where only current peaks cause firing. In this case, the firing domain is very narrow and differentiated, but the probability of firing becomes negligible.

A neuron with different morphology, or different biophysical properties, which has significantly slower propagation speeds across its dendritic tree, would likely be able to distinguish input time delays at much higher precision. Given the neuron used in this study, as long as it fires at a reasonable rate (i.e., the firing probability is not extremely low), the neuron shows little sensitivity to fluctuations in input time delays on the order of the effective width of the EPSP.

Acknowledgements

We are grateful to the three anonymous referees for their constructive and stimulating comments.

References

Bi, G.-Q., Poo, M.-M., 1998. Synaptic modifications in cultured hippocampal neurons: dependence on spike timing, synaptic strength, and postsynaptic cell type. Journal of Neuroscience 18 (24), 10464–10472.

Branco, T., Clark, B. A., Häusser, M., 2010. Dendritic discrimination of temporal input sequences in cortical neurons. Science 329 (5999), 1671–1675.

Bugmann, G., Christodoulou, C., 2001. Learning temporal correlation between input neurons by using dendritic propagation delays and stochastic synapses. In: Proceedings of the International Workshop on Neural Coding. Plymouth, UK, pp. 131–132.

Dan, Y., Poo, M.-M., 2004. Spike timing-dependent plasticity of neural circuits. Neuron 44 (1), 23–30.

Deisz, R. A., Fortin, G., Zieglgansberger, W., 1991. Voltage dependence of excitatory postsynaptic potentials of rat neocortical neurons. Journal of Neurophysiology 65 (2), 371–382.

Denham, M. J., Denham, S. L., 2001. A synaptic learning rule based on the temporal coincidence of pre- and postsynaptic activity. In: Proceedings of

the International Joint Conference on Neural Networks (IJCNN'01). Vol. 1 Jul 2001. Washington D.C., USA, pp. 1–6.

Destexhe, A., Paré, D., 1999. Impact of network activity on the integrative properties of neocortical pyramidal neurons in vivo. Journal of Neurophysiology 81, 1531–1547.

Eurich, C. W., Pawelzik, K., Ernst, U., Thiel, A., Cowan, J. D., Milton, J. G., 2000. Delay adaptation in the nervous system. Neurocomputing 32-33, 741–748.

Fricker, D., Miles, R., 2000. EPSP amplification and the precision of spike timing in hippocampal neurons. Neuron 28 (2), 559–569.

Froemke, R. C., Dan, Y., 2002. Spike-timing-dependent synaptic modification induced by natural spike trains. Nature 416, 433–438.

Gerstner, W., Kempter, R., Hemmen, J. L. V., Wagner, H., 1998. Hebbian Learning of Pulse Timing in the Barn Owl Auditory System. In: Maass, W., Bishop, C. M. (Eds.), Pulsed Neural Nets. MIT Press, Cambridge, MA, Ch. 14, pp. 353–377.

González-Burgos, G., Barrionuevo, G., 2001. Voltage-gated sodium channels shape subthreshold EPSPs in layer 5 pyramidal neurons from rat prefrontal cortex. Journal of Neurophysiology 86 (4), 1671–1684.

Häusser, M., 2001. Synaptic function: Dendritic democracy. Current Biology 11 (1), R10–R12.

Hines, M., Carnevale, T., 1997. The NEURON simulation environment. Neural Computation 9 (6), 1179–1209.

Hüning, H., Glünder, H., Palm, G., 1998. Synaptic delay learning in pulse-coupled neurons. Neural Computation 10, 555–565.

Hunzinger, J. F., Chan, V. H., Froemke, R. C., 2012. Learning complex temporal patterns with resource-dependent spike timing-dependent plasticity. Journal of Neurophysiology 108 (2), 551–566.

Kampa, B. M., Clements, J., Jonas, P., Stuart, G. J., 2004. Kinetics of Mg2+ unblock of NMDA receptors: implications for spike-timing dependent synaptic plasticity. Journal of Physiology 556 (Pt 2), 337–345.

Kerr, R. R., Burkitt, A. N., Thomas, D. A., Gilson, M., Grayden, D. B., 2013. Delay selection by spike-timing-dependent plasticity in recurrent networks of spiking neurons receiving oscillatory inputs. PLoS Computational Biology 9 (2), e1002897.

Letzkus, J. J., Kampa, B. M., Stuart, G. J., 2006. Learning rules for spike timing-dependent plasticity depend on dendritic synapse location. Journal of Neuroscience 26 (41), 10420–10429.

Markram, H., Lübke, J., Frotscher, M., Sakmann, B., 1997. Regulation of synaptic efficacy by coincidence of postsynaptic APs and EPSPs. Science 275 (5297), 213.

Marom, S., Shahaf, G., 2002. Development, learning and memory in large random networks of cortical neurons: lessons beyond anatomy. Quarterly Reviews of Biophysics 35 (1), 63–87.

Pun, R. Y., Neale, E. A., Guthrie, P. B., Nelson, P. G., 1986. Active and inactive central synapses in cell culture. Journal of Neurophysiology 56 (5), 1242–1256.

Redman, S., 1990. Quantal analysis of synaptic potentials in neurons of the central nervous system. Physiological Reviews 70 (1), 165–98.

Saul, A. B., 2008. Lagged cells in alert monkey lateral geniculate nucleus. Visual Neuroscience 25 (5-6), 647–59.

Senn, W., Schneider, M., Ruf, B., 2002. Activity-Dependent Selection of Axonal and Dendritic Delays Or, Why Synaptic Transmission Should Be Unreliable. Neural Computation 14 (3), 583–619.

Spruston, N., 2008. Pyramidal neurons: dendritic structure and synaptic integration. Nature Reviews Neuroscience 9, 206–221.

Stuart, G., Sakmann, B., 1995. Amplification of EPSPs by axosomatic sodium channels in neocortical pyramidal neurons. Neuron 15 (5), 1065–1076.

Stuart, G. J., Spruston, N., 1998. Determinants of voltage attenuation in neocortical pyramidal neuron dendrites. Journal of Neuroscience 18 (10), 3501–3510.

van Leeuwen, M., 2004. Spike timing dependent structural plasticity in a single model neuron. Tech. Rep. INF/SCR-04-15, Institute for Information and Computing Sciences, Utrecht University.

Zhang, L. I., Tao, H. W., Holt, C. E., Harris, W. A., Poo, M.-M., 1998. A critical window for cooperation and competition among developing retinotectal synapses. Nature 395, 37–44.

Zsiros, V., Hestrin, S., 2005. Background synaptic conductance and precision of EPSP-spike coupling at pyramidal cells. Journal of Neurophysiology 93 (6), 3248–3256.